Onset of Excluded-Volume Effects in Chain Dynamics

H. Sahouani† and T. P. Lodge*

Department of Chemistry, University of Minnesota, Minneapolis, Minnesota 55455

Received January 21, 1992; Revised Manuscript Received July 8, 1992

ABSTRACT: The infinite-dilution oscillatory flow birefringence properties of five high molecular weight polybutadienes (M = 3.55 × 10^5, 9.25 × 10^5, 2.95 × 10^6, 3.74 × 10^6, and 1.6 × 10^7) have been determined in dioctyl phthalate at 18.0, 21.5, 25.0, and 30.0 °C. The Θ temperature for this system has been estimated as 21.5 °C, and thus the results extend from the Θ into the marginal solvent regime. For each temperature, the data for the five molecular weights are superposed to form master curves. The resulting plots are equivalent, via the stress-optical relation, to plots of the reduced intrinsic shear moduli, $[G'_P]_R$ and $[G''_P]_R$, versus reduced frequency, $\omega\tau_1$, where τ_1 is the longest relaxation time. For 18 and 21.5 °C, the master curves are precisely described by the bead–spring model (BSM) with the hydrodynamic interaction parameter, h^*, equal to 0.25. At 30 °C, however, effects attributable to excluded volume are apparent. At this temperature, the data are compared with five approximate but distinct approaches to incorporating excluded volume: the Gaussian BSM with variable h^*; dynamic scaling; the non-Gaussian BSM with h^* equal to 0.25 and incorporating chain expansion via the uniform expansion model, the blob model, or the renormalization group. All five methods can be used to describe the frequency dependence of the reduced intrinsic moduli very well but differ in their ability to describe the chain expansion concurrently. In particular, the renormalization group approach is as good or better than the other models, and thus the success of the BSM coupled with the renormalization group establishes an effective theoretical framework for describing quantitatively both the static and dynamic properties of isolated flexible chains.

Introduction

The influence of intrachain excluded-volume interactions on the conformational dynamics of flexible polymer chains remains to be completely elucidated. The coupling between chain expansion and the strength of the hydrodynamic interactions presents difficulties from both an experimental and a theoretical perspective. However, modern instrumentation permits precise determination of the infinite-dilution oscillatory flow birefringence (OFB) or linear viscoelastic (VE) properties of high molecular weight chains over a sufficient range of frequency and in solvents of varying quality that these questions may be addressed. Concurrently, the incorporation of renormalization group (RG) calculations of intrachain distances into the bead–spring model (BSM) leads to explicit predictions for the effect of solvent quality on the spectrum of relaxation times, in a manner which may ultimately succeed in unifying the description of both static and dynamic properties.

The BSM, as developed by Rouse[1] and Zimm,[2] ignores excluded-volume interactions, resulting in a Gaussian segment distribution for long chains; it is thus presumed to be most applicable in the vicinity of the Θ temperature. Traditionally, two approaches have been taken to describe the conformational dynamics of polymers in solvents of intermediate or good quality. In one, first proposed by Ptitsyn and Eizner,[3] the elements of the Zimm **H·A** matrix (the eigenvalues of which are inversely proportional to the relaxation times of the model chain) are modified to account for solvent quality-dependent changes in the average inverse bead separation $\langle r_{ij}^{-1}\rangle$. The calculation of $\langle r_{ij}^{-1}\rangle$ may be undertaken in various ways. For example, the uniform expansion model of Peterlin[4] was employed by Tschoegl,[5] whereas the RG calculations of Miyake and Freed[6] were incorporated by Sammler and Schrag.[7] It is important to emphasize that the Ptitsyn–Eizner formalism is still approximate, in the sense that the equations of motion for the beads along the chain do not contain an explicit uncrossability constraint. The second approach, first advanced by Thurston and co-workers,[8] modifies the **H·A** matrix simply by varying the value of the hydrodynamic interaction parameter, h^*. Empirically, it has been demonstrated extensively that the resulting changes in the relaxation time spacings describe the chain dynamics properties very well.[9-14] However, this approach offers no fundamental connection between the effects of excluded volume, which are manifest in both static and dynamic properties, and the strength of the hydrodynamic interaction.

Experimentally, the infinite dilution VE and OFB properties of polystyrenes in Aroclor solvents have been examined in detail, as functions of molecular weight and chain branching.[10-17] The viscosity of an Aroclor is an extremely strong function of temperature, which enables examination of dynamics over a wide range of time scales via time–temperature superposition. Furthermore, the high solvent viscosities bring the chain dynamics into the experimentally accessible frequency range. However, Aroclors are moderately good solvents for polystyrene, and therefore the solvent quality cannot be varied appreciably by varying temperature (indeed, this must be the case for the application of time–temperature superposition). Nevertheless, some insight into the effect of solvent quality on the VE properties of polystyrenes has been gained by use of other solvents, whereas, to our knowledge, no infinite dilution OFB properties of polymers in non-Aroclor solvents have been reported previously, although an extensive series of OFB measurements on dilute solutions of a high molecular weight polystyrene in styrene oligomer have been completed.[18] Johnson et al.[19] determined the infinite dilution VE properties of a high molecular weight polystyrene in moderately good solvents (Aroclor 1232 and α-chloronaphthalene) and Θ solvents (decalin and dioctyl phthalate); the effective frequency range was extended by use of solvent pairs with substantially different viscosities. Prior to this, the infinite dilution VE properties of poly(α-methylstyrene) in a Θ solvent and a good solvent were reported by Tanaka et al.[20] In both cases, the results were reasonably well-

* Author to whom correspondence should be addressed.
† Current address: 3M Company, 3M Center, St. Paul, MN 55144-1000.

0024-9297/92/2225-5632$03.00/0

Table I
Sample Characteristics

M_w	M_w/M_n	% 1,4-cis	% 1,4-trans	% 1,2
3.55×10^5	1.09	40	51	9
9.25×10^5	1.09	45	46	9
2.95×10^6	<1.1	39	46	15
3.74×10^6	<1.1	58	35	7
1.60×10^7	<1.1	66	25	9

described by the BSM with excluded volume incorporated via the Tschoegl approach.[5] More recently, Hair and Amis[21,22] have reported extensive and precise infinite dilution VE properties for polystyrenes with a range of molecular weights in the good solvent toluene and the Θ solvent decalin and compared these results with the modified BSM approaches identified above, as well as with the dynamic scaling predictions of Doi and Edwards.[23] In their work, the effective frequency range was increased by use of a range of high molecular weights (1.8×10^5–2×10^7).

The effective frequency range accessed by the experimental technique is an important consideration, as it is the effects of excluded volume on the internal modes that are of interest here, and such effects should be most evident at high effective frequency. The VE results of Johnson et al.[19] and Amis and Hair[21,22] were obtained with versions of the multiple-lumped resonator (MLR) apparatus developed by Birnboim and Schrag.[24] This instrument provides measurements of the storage and loss shear moduli, G' and G'', respectively, at five discrete resonance frequencies spread over a factor of approximately 60. One possible advantage of the OFB approach is the ability to select any measurement frequency over a range from approximately 0.1 to 1000 Hz. However, for dilute solutions the OFB experiment is restricted to polymer/solvent systems that are nearly isorefractive, to minimize form birefringence effects, which eliminates the possibility of light scattering measurements on the same solutions. In addition, the strength of the signal for a given polymer depends on the stress-optic coefficient, and thus the lowest solution concentration that can be measured reliably depends on the chemical identity of the polymer.

In this work we report the infinite dilution OFB properties for five high molecular weight polybutadienes in dioctyl phthalate (DOP). This system was reported to have a Θ temperature near 21.5 °C,[25,26] and we present results at 18, 21.5, 25, and 30 °C. At the highest temperature, the onset of excluded-volume effects is clearly evident. The data are interpreted in terms of the BSM incorporating five distinct approaches to treating excluded-volume interactions. These are (i) the Gaussian BSM with variable hydrodynamic interaction; the non-Guassian BSM, with $\langle r_{ij}^{-1} \rangle$ given variously by (ii) the uniform expansion model, (iii) the "blob" model, or (iv) the chain-space renormalization group calculation; and (v) the dynamic scaling approach.

Experimental Section

A. Samples and Solutions. The molecular weights, polydispersities, and microstructures of the polybutadiene (PB) samples are listed in Table I. The details of the characterization have been presented elsewhere;[27] the samples were generously provided by Dr. R. H. Colby (sample 1) and Dr. L. J. Fetters (samples 2–5). The solvent, bis(2-ethylhexyl phthalate) (dioctyl phthalate; DOP), was obtained from Aldrich, with a purity of 98%. The DOP was neutralized with a 4% solution of sodium bicarbonate, dried over calcium chloride, and distilled under vacuum; it was stored in a vacuum desiccator. The viscosity of DOP is 0.849, 0.713, 0.581, and 0.412 P at temperatures of 18, 21.5, 25, and 30 °C, respectively. Initial solutions were prepared gravimetrically by direct addition of DOP to the PB, with approximately 50% by weight of benzene added as a cosolvent to assist dissolution. The benzene was subsequently stripped off under vacuum, after which a small but insignificant weight loss of approximately 1 mg/25 g of solution was observed. Each solution also contained 0.1% by weight of PB of butylhydroxytoluene (BHT) as an antioxidant. After each initial solution was prepared and OFB measurements were completed, subsequent concentrations were prepared by direct dilution. The concentrations employed are listed in Table II; concentrations were converted to g/mL assuming additivity of volumes and densities of 0.895 and 0.981 g/mL for PB and DOP, respectively. All solutions were stored under vacuum, at ambient temperature, and in the dark. The integrity of one of the samples ($M = 9.25 \times 10^5$) was checked prior to and after the OFB measurements were completed, by size-exclusion chromatography; no evidence of degradation was detected.

Table II
Solution Concentrations

c (mg/mL)	c[η]	c (mg/mL)	c[η]
	$M_w = 3.55 \times 10^5$		
4.9	0.39	16.5	1.33
7.0	0.56	18.5	1.49
9.0	0.73	20.6	1.66
11.2	0.90	23.2	1.87
14.2	1.14		
	$M_w = 9.25 \times 10^5$		
4.0	0.59	6.9	1.01
4.9	0.72	7.8	1.14
5.9	0.87	9.4	1.38
	$M_w = 2.95 \times 10^6$		
1.5	0.39	3.1	0.80
1.9	0.49	3.9	1.00
2.3	0.59	4.7	1.21
	$M_w = 3.74 \times 10^6$		
1.5	0.42	4.9	1.38
1.9	0.53	5.9	1.66
2.5	0.70	7.9	2.22
2.9	0.81	10.8	3.03
3.9	1.10		
	$M_w = 1.60 \times 10^7$		
0.30	0.18	1.2	0.72
0.60	0.36	1.7	1.03
0.80	0.49	2.2	1.33

B. Oscillatory Flow Birefringence Measurements. The oscillatory flow birefringence (OFB) apparatus, measurement procedure, and data acquisition algorithm have been discussed in detail elsewhere.[14,16,28,29] The optical train consists of a diode laser, linear polarizer, quarter-wave plate, sample, beam-splitting polarizer, and dual photodiode detectors. The diode laser (Sharp Electronics) replaces the HeNe laser of the previous design[14] to achieve greater intensity stability. It provides approximately 5 mW at a wavelength of 785 nm. It is mounted on a home-built thermal regulator, and the emitted radiation is collimated by a microscope objective and lens combination. The advantages of the dual photodetectors, one to monitor each polarization component, have been discussed elsewhere.[14,29] The sample solution is confined to a thin layer (0.227 mm) between a fixed (stainless steel) block and a moving (black glass) surface. The oscillatory shear is generated by a thin fluid layer transducer which follows the Miller–Schrag design;[14,28] the measurement frequency range extends from 0.1 to 1000 Hz. The data acquisition and processing algorithm, to extract the relative magnitudes and phases of the two optical signals and the velocity of the moving plane, has been described in detail elsewhere.[16,29] Solution temperatures were controlled to ±0.01 °C and monitored by a thermistor calibrated to ±0.003 °C, with a calibration traceable to NIST.

Results and Discussion

I. Extraction of Infinite-Dilution Chain Dynamics Properties. The OFB data may be presented in terms

of the complex mechanooptic coefficient, S^*, defined as the ratio of the sinusoidally time-varying briefringence (Δn^*) to the sinusoidally time-varying shear rate ($\dot{\gamma}^*$). Thus, one may write

$$S^* \equiv \Delta n^*/\dot{\gamma}^* = S' + iS'' = S_m \exp(i\theta) \quad (1)$$

where S' and S'' are the in-phase (viscous) and out-of-phase (elastic) components, respectively; S_m is the magnitude and θ the phase angle between the birefringence and the shear rate. In this work the data are reported in terms of S' and S'', rather than in the more commonly employed polar format,[10-17,28] in order to generate master curves by superposing data for different molecular weights.

The measured solution properties include contributions from both polymer and solvent, and, over the range of concentrations and frequencies examined here, the solvent contributes only to the viscous component. The polymer contributions are thus obtained as

$$S'_P = S'_{sol,n} - S_e \quad (2a)$$

$$S''_P = S''_{sol,n} \quad (2b)$$

where the subscript P denotes the polymer contribution, and S_e refers to the contribution of the environment solvating the chain. Traditionally, S_e has been taken as $\phi_s S_s$, where ϕ_s is the solvent volume fraction and S_s is the magnitude of the birefringence for the neat solvent.[10-16,28] However, recently it has been demonstrated conclusively that the presence of polymer can modify the dynamics of the solvent in the vicinity of the chain and that in general this subtraction procedure is at best approximate.[12-14,17,30-35] The same conclusion may be drawn in the case of the VE properties; i.e., the solvent contribution is not generally equal to the neat solvent viscosity, η_s.[18,31-36] Nevertheless, in this work we adopt the traditional solvent subtraction approach (i.e., $S_e = \phi_s S_s$), for two reasons. First, in this situation we feel that the resulting error is insignificant, and, second, we have no independent means to quantify any difference between S_e and $\phi_s S_s$. The assumption of insignificant error is supported by several factors. First, the measurements were all made at low concentrations, where the effect is small, and then extrapolated to infinite dilution; the extrapolation process largely eliminates the difficulty. Second, if there were a substantial difference between S_e and $\phi_s S_s$, then there would be significant differences between experimental values of S'_P and theoretical curves at high frequency, even when the theoretical curves were generated in such a way as to describe S''_P well. Such differences are not observed, as will be evident in the subsequent discussion. Finally, OFB measurements were made on a 2.7% by weight solution of a butadiene oligomer (M = 900; Polymer Laboratories, Inc.) in DOP. Previously, differences between S_e and $\phi_s S_s$ have been shown to be substantially independent of M, and thus any changes in the solvent contribution are more readily apparent at very low M, where the polymer contribution is greatly reduced. For the oligomer concentration examined, which is greater than any employed for the higher M samples, the difference between $S'_{sol,n}$ and S_s was less than 10%, thus supporting the conclusion that the presence of PB has at most a modest effect on S_e. For the highest c solution of the highest M examined, this could result in at most a 0.25% error in the values of S'_P at high frequencies. It is exactly these data that are the most important in the analysis to follow.

The OFB data can be compared to the predictions for the VE properties via the stress-optical relation (SOR).

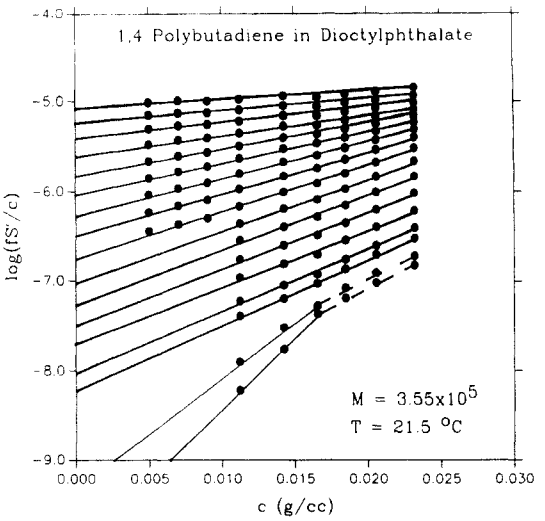

Figure 1. Extrapolation to infinite dilution for the in-phase dynamic birefringence at selected drive frequencies, for M = 3.55×10^5 and T = 21.5 °C. From the top of the plot, the data sets correspond to drive frequencies of 251.2, 199.9, 158.5, 101.1, 82.10, 63.10, 39.81, 25.12, 15.80, 10.11, 6.31, 3.98, 2.51, 1.58, 1.01, 0.63, and 0.39 Hz, respectively.

The SOR is embodied in two postulates, namely, that the refractive index tensor and the stress tensor have (i) identical principal axes, resulting in identical extinction and stress orientation angles, and (ii) proportional differences in principal values. Thus, we can write

$$S^*_P = 2C\eta^*_P \quad (3a)$$

$$S'_P = 2C\eta'_P = 2CG''_P/\omega \quad (3b)$$

$$S''_P = -2C\eta''_P = -2CG'_P/\omega \quad (3c)$$

where η' and η'' are the viscous and elastic components of the dynamic shear viscosity, η^*, G'' and G' are the viscous and elastic components of the dynamic shear modulus, G^*; ω is the driving frequency in rad/s, and C is the stress-optic coefficient. There is extensive evidence that the SOR is obeyed for solutions and melts of flexible homopolymers.[37]

The finite concentration data were extrapolated to infinite dilution via linear regression fits of log (fS'_P/c) and log (fS''_P/c) versus c, where f is the drive frequency in Hz and c is the concentration in g/mL. Multiplication by f anticipates that the resulting intrinsic quantities (i.e., the c = 0 intercepts) [fS'_P] and [fS''_P] will be proportional to [G''_P] and [G'_P], respectively, via the SOR. The OFB data may be extrapolated to infinite dilution in a variety of different formats, with entirely equivalent results;[10] however, the use of the logarithm effectively linearizes the data over the c range examined. For the lowest M examined, the data extend over the range $0.39 < c[\eta] < 1.14$, whereas for the highest M, the corresponding interval is $0.18 < c[\eta] < 1.0$. Typical examples of the extrapolations are shown in Figures 1 and 2.

II. Theoretical Predictions for [fS'_P] and [fS''_P].

A. Bead-Spring Model with Variable Hydrodynamic Interaction. The BSM represents an isolated polymer molecule as a linear chain of $N + 1$ beads, each with a friction coefficient ζ, connected by N Hookean springs, each with root-mean-square length b, embedded in a Newtonian continuum of viscosity η_e.[1,2] The use of η_e in place of η_s, the viscosity of the neat solvent, explicitly acknowledges the possibility that the presence of the chain affects the dynamics of the solvent. The resulting

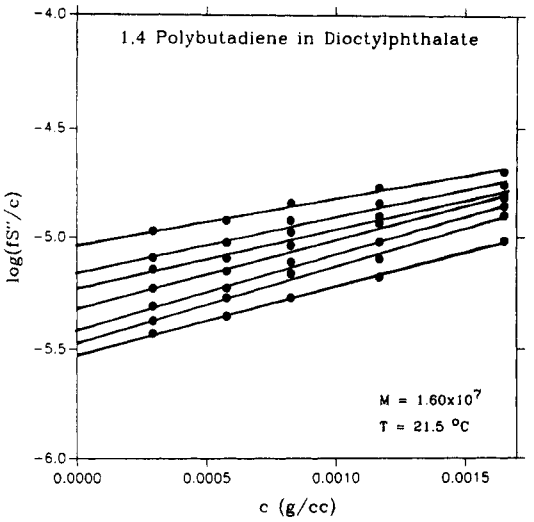

Figure 2. Extrapolation to infinite dilution for the out-of-phase dynamic birefringence at selected drive frequencies, for $M = 1.6 \times 10^7$ and $T = 21.5$ °C. From the top of the plot, the data sets correspond to drive frequencies of 199.9, 158.5, 125.9, 101.1, 82.10, 63.10, and 50.11 Hz, respectively.

predictions for the intrinsic VE properties are

$$[G'_p] = (RT/M)\sum_k [\omega^2\tau_k^2/(1+\omega^2\tau_k^2)] \quad (4a)$$

$$[G''_p] = (RT/M)\sum_k [\omega\tau_k/(1+\omega^2\tau_k^2)] \quad (4b)$$

where R is the gas constant, T is the absolute temperature, and the $\{\tau_k, k = 1, ..., N\}$ are the relaxation times associated with the N normal modes. The reduced intrinsic moduli are defined as

$$[G'_p]_R \equiv (M/RT)[G'_p] = \sum_k [\omega^2\tau_k^2/(1+\omega^2\tau_k^2)] \quad (5a)$$

$$[G''_p]_R \equiv (M/RT)[G''_p] = \sum_k [\omega\tau_k/(1+\omega^2\tau_k^2)] \quad (5b)$$

and depend only on the relaxation times. The N relaxation times are determined from the nonzero eigenvalues of the Zimm **H·A** matrix, λ_k, by

$$\tau_k = (b^2\zeta/6k_BT\lambda_k) \quad (6)$$

where k_B is the Boltzmann constant. The eigenvalues depend only on N and the hydrodynamic interaction parameter, h^*, defined as

$$h^* \equiv \zeta/[(12\pi^3)^{0.5}b\eta_e] \quad (7)$$

and thus the spacings of the relaxation times, and the shapes of the frequency dependences of the reduced intrinsic moduli, also depend only on N and h^*. However, the magnitude of the longest relaxation time, τ_1, requires independent specification of ζ and b.

The exact eigenvalues can be computed numerically for arbitrary values of N and h^* via the highly efficient computer algorithm developed by Sammler and Schrag.[7] This algorithm is based on the one designed by Lodge and Wu,[38] in which the $(N+1) \times (N+1)$ singular **H·A** matrix is replaced by the nonsingular, symmetric $N \times N$ **B** matrix, through the transformation to normal coordinates (preserving the internal modes only). For this work only the off-diagonal elements of the hydrodynamic interaction matrix, **H**, are of concern; the reader is referred to the work of Sammler and Schrag[7] for more details on the computation. These elements may be written as

$$H_{ij} = (\zeta/6\pi\eta_e)\langle r_{ij}^{-1}\rangle = (h^*b(\pi/3)^{0.5})\langle r_{ij}^{-1}\rangle \quad (8)$$

The quantity $\langle r_{ij}^{-1}\rangle$ arises from the inclusion of the hydrodynamic interaction following the Kirkwood–Riseman formalism,[39] i.e., with an equilibrium preaveraged Oseen tensor. For a Gaussian chain

$$\langle r_{ij}^{-1}\rangle = (\langle r_{ij}^2\rangle\pi/6)^{-0.5} = (6/\pi)^{0.5}/(b|i-j|^{0.5}) \quad (9)$$

with $\langle r_{ij}^2\rangle = b^2|i-j|$.

The values of h^* range from 0.25, in the non-free-draining or Zimm limit, down to 0, in the free-draining or Rouse limit. Empirically, under Θ conditions the dynamics have been found to be well-described by the BSM with $h^* = 0.25$, whereas in solvents of increasing quality, lower values of h^* are required to reproduce the frequency dependence of the reduced intrinsic moduli. For example, for polystyrenes in Aroclor 1248, a moderately good solvent (vide infra), a value of $h^* \approx 0.15$ has been deduced,[10-14] whereas in the good solvent toluene, $h^* \approx 0.04$ was obtained.[21] The general result that an increase in coil dimensions leads to a reduction in the strength of the hydrodynamic interaction is plausible, but it is important to emphasize that varying h^* is an ad hoc procedure for modifying the spacings among the relaxation times. Taken literally, for example, it would imply that the ratio $\zeta/b\eta_e$ decreases by over a factor of 5 in going from a Θ solvent to a good solvent. Given that the bead exhibits a Stokes law friction, $\zeta \sim r\eta_e$, where r is the bead radius, it further implies that either the ratio r/b decreases by the same factor, which is implausible, or that the application of Stokes law is inappropriate. In addition, the quantity $\langle r_{ij}^{-1}\rangle$, which is known to change with solvent power, remains unchanged (unless an explicit change in b is incorporated). Thus, although the use of a variable h^* to account for changes in solvent quality is generally able to reproduce the changes in the frequency dependences of the reduced intrinsic moduli and although it has the virtue of maintaining the BSM as a three-parameter model (i.e., N, b, and ζ), the physical interpretation of the results is inherently unsatisifying.

B. Inclusion of Excluded Volume in the Ptitsyn–Eizner Formalism. Ptitsyn and Eizner were the first to incorporate excluded volume into the BSM in an approximate way, by modifying the expression for $\langle r_{ij}^{-1}\rangle$.[3] In the following, we consider three distinct models for this quantity: (i) the uniform expansion model of Peterlin,[4] as applied by Tschoegl;[5] (ii) a modified "blob" model, building on the treatments of Daoud and Farnoux et al.[40] and Akcasu and co-workers;[41] and (iii) the renormalization group calculations of Miyake and Freed.[6]

(i) Uniform Expansion. Peterlin[4] proposed that the effect of excluded volume could be approximated by assuming that the degree of expansion was independent of molecular weight; specifically

$$\langle r_{ij}^2\rangle = \alpha^2 b_0^2|i-j|^{1+\epsilon} \quad (10)$$

Here, α is the chain expansion parameter, ϵ is a temperature-dependent exponent, and b_0 is the value of b under Θ conditions (where $\alpha = 1$ and $\epsilon = 0$). As the spacings among the relaxation times are independent of the value of b, independent specification of b_0 and α is not usually attempted. To incorporate this expression in eq 8, an additional approximation is necessary:

$$\langle r_{ij}^{-1}\rangle = (\langle r_{ij}^2\rangle\pi/6)^{-0.5} \quad (11)$$

which is strictly valid only for Gaussian chains.

As developed in detail by Tschoegl,[5] this form of the BSM has been shown to describe the VE properties of flexible chains rather well. It has also been demonstrated that very similar changes in the relaxation time spacings can be achieved by varying h^* alone (with $\epsilon = 0$), and as there was generally no independent means to determine ϵ, the variable h^* approach has been more commonly employed. However, there is a more fundamental objection to the use of eq 10. It is well established, both theoretically and experimentally, that coil expansion is not uniform and that excluded-volume effects are more important on longer length scales. This is particularly important in the case of marginal solvents, which may appear to be Θ-like for relatively low molecular weight chains but quite good for very high molecular weights.

(ii) Modified Blob Model. The inapplicability of the uniform expansion approach to global chain properties such as the radius of gyration, diffusion coefficient, and intrinsic viscosity led to the development of the so-called blob model,[40] in which the length-scale dependence of coil expansion is explicitly recognized. In its original form, the expression for the average intrachain distances could be written

$$\langle r_{ij}^2 \rangle = b^2 N_\tau^{(1-2\nu)} |i-j|^{2\nu} \tag{12}$$

where $\nu = 0.5$ for $|i-j| \leq N_\tau$ and 0.6 for $|i-j| > N_\tau$, and N_τ is a temperature-dependent cutoff between Θ dimensions for small $|i-j|$ and fully-developed excluded volume for large $|i-j|$.[40] An advantage of this approach is that the temperature dependence of the chain dimensions is incorporated through the relation

$$N_\tau = A(1 - T/T_\Theta)^{-2} \tag{13}$$

where T_Θ is the Θ temperature, and A is a system-dependent parameter to be determined empirically. For a Θ solvent, $N_\tau \to \infty$, whereas in a good solvent $N_\tau \to 1$. This should be contrasted with the uniform expansion approach, in which ϵ is increases monotonically with T from 0 at the Θ condition to 0.2 in a good solvent (not the limit of 0.33 originally suggested), but in an unspecified manner. A serious difficulty with the blob approach, aside from its origin as a postulate, is the unphysical abrupt cutoff at $N = N_\tau$. However, this may be overcome by use of a modification suggested by Akcasu et al.,[41] in which eq 12 is replaced by

$$\langle r_{ij}^2 \rangle = \alpha_{ij}^2 b^2 |i-j| \tag{14}$$

where α_{ij} is a local swelling factor given by

$$\alpha_{ij}^5 - \alpha_{ij}^3 = (|i-j|/N_\tau)^{0.5} \tag{15}$$

by analogy to Flory's result.[42]

The incorporation of the blob model (in either form) in eq 8 also requires the Gaussian assumption in obtaining the inverse first moment from the second moment of the distribution function. In general, the predictions for $\{\tau_k\}$ using eqs 12 and 13 do not differ significantly from those obtained via eqs 14 and 15, at least for $h^* = 0.25$. Furthermore, the results are quite similar to those obtained via the uniform expansion approach. This underscores the relative insensitivity of the internal modes of the chain to the details of how the excluded-volume interaction is taken into account. One interesting feature does emerge, however, for low values of N_τ (e.g, $N_\tau < 50$); some of the eigenvalues of the **H·A** matrix were found to be negative. A similar result can be obtained from the Gaussian BSM with variable h^* if this parameter is allowed to exceed approximately 0.25. This observation has been reconciled by Osaki[43] in the context of a modified version of Zimm's original integrodifferential equation for the eigenvectors, whereby a prefactor equal to $1 - 4h^*$ appears. Using the blob model and following Osaki's approach, the corresponding prefactor becomes $1 - 4.90h^*$, suggesting that h^* be maintained below 0.204 to ensure that all eigenvalues remain positive. Incorporation of this restriction does eliminate the problem, but it is important to note that for $|i-j| < N_\tau$, i.e., for length scales where Gaussian statistics apply, the value of h^* was retained as 0.25, to ensure convergence to the original BSM in a Θ solvent. In other words, two values of h^* may be required in this formalism.

(iii) Renormalization Group. Sammler and Schrag[7] have adapted the chain conformation space renormalization group (RG) calculations of Miyake and Freed[6] for the effect of excluded volume on the intermonomer distances in a regular star polymer to the BSM calculations of $\{\tau_k\}$, within the Ptitsyn–Eizner framework.[3] In general the RG approach provides much more rigorous and explicit predictions for the temperature dependence of chain properties than either of the ad hoc methods described previously, at the cost of considerable complexity. The Miyake–Freed model,[6] although developed for stars, is applicable to linear polymers (two-armed stars) as they fall in the same universality class. Indeed, this treatment is expected to be better for small numbers of arms, f, (i.e., $f < 6$–7), due to the neglect of monomer–monomer packing constraints near the star center. Sammler and Schrag's calculations also indicate that the complete range of solvent quality is accessible via this method.[7] As originally derived[6] and as incorporated by Sammler and Schrag,[7] the resulting predictions for $\langle r_{ij}^{-1} \rangle$ depend on two additional parameters: a dimensionless scaling variable, ζ_{RG} (related to the traditional z parameter[44]), that varies from 0 in a Θ solvent to ∞ for an infinite chain in a very good solvent, and a crossover length scale, L, that may be considered as equivalent to N_τ in the blob model. Without an independent means to establish the appropriate values of L and ζ_{RG}, therefore, the fact that this model can describe the data as well as the others is neither surprising nor particularly enlightening. Amis and Hair, for example, showed that the infinite-dilution VE properties of polystyrene in toluene were well-described with $\zeta_{RG} = 1000$ and $L = b$ and h^* fixed at the nondraining limit of 0.25.[22]

More recently, Freed[45] has demonstrated that the Miyake–Freed results for $\langle r_{ij}^{-1} \rangle$ can be recast by comparison with the results of Douglas and Freed[46] for the dimensions of a linear chain, in such a way that L is scaled out of the problem, and ζ_{RG} is replaced by $6.44z$. In other words, the effects of excluded volume may be incorporated into the BSM at the cost of only one additional parameter, which may be estimated independently through the temperature dependences of the intrinsic viscosity, the radius of gyration, or the diffusivity. The resulting expressions for the average interbead separations are[6,7,45-48]

$$\langle r_{ij}^{-1} \rangle = (12/\pi N b^2)^{0.5}[(1 + 6.44z) + 6.44z(1 + 6.44z)^{15/32}]^{-1/8}(x-y)^{-\nu} \exp\{0.805z(A+B)/(1+6.44z)\} \tag{16}$$

for beads on the same branch, and

$$\langle r_{ij}^{-1} \rangle = (12/\pi N b^2)^{0.5}[(1 + 6.44z) + 6.44z(1 + 6.44z)^{15/32}]^{-1/8}(x+y)^{-\nu} \exp[0.805z(A')/(1+6.44z)] \tag{17}$$

for beads on opposite branches. In these expressions x and y refer to the fractional length along the branch from the center of the chain, so that $x = 2i/N$ and $y = 2j/N$. The quantities A, B, and A' are complicated functions of x and

y that are presented elsewhere.[7] The exponent ν is well approximated by

$$\nu = 0.5[1 + (0.805z/(1 + 6.44z)) + (15/256)(6.44z/[1 + 6.44z])^2] \quad (18)$$

In eqs 16 and 17, the dimensionality has been fixed as $d = 3$, the RG expansion parameter as $\epsilon = 4 - d = 1$, and the number of arms as $f = 2$, and the numerical front factor incorporates a Gaussian result which is 7% larger than the RG value.[7]

C. Dynamical Scaling. In this approach the scaling arguments that appear to represent the static behavior of high molecular weight chains very well[49] are extended directly to the dynamic case;[23] the primary result is that

$$\tau_k = \tau_1 k^{-3\nu} \quad (19)$$

where ν is the excluded-volume exponent. This relation presupposes a Zimm chain, i.e., $h^* > 0$, as is appropriate for infinite dilution. Substitution of eq 19 into eqs 5a and 5b (with $N \to \infty$) leads directly to absolute predictions for the reduced moduli as functions of reduced frequency $\omega\tau_1$, which may be compared with the data for high molecular weight chains. The most interesting feature of these predictions occurs in the regime $\omega\tau_1 \gg 1$, where

$$[G'_P]_R = (\omega\tau_1)^{1/3\nu}(\pi/6\nu \sin(\pi/6\nu)) \quad (20a)$$

$$[G''_P]_R = (\omega\tau_1)^{1/3\nu}(\pi/6\nu \cos(\pi/6\nu)) \quad (20b)$$

In addition to the magnitudes, therefore, the scaling approach predicts that both moduli scale with the same power of frequency. For a Θ solvent this slope would be $^2/_3$, the well-known result for the Zimm chain. For a good solvent with $\nu = 0.59$, the slope would be 0.565.

III. Infinite-Dilution Results and Comparison with Theory. The intrinsic OFB properties, $[fS'_P]$ and $[fS''_P]$, have been obtained as functions of frequency for each of the five samples, and each at four temperatures (18.0, 21.5, 25.0, and 30.0 °C). In order to superpose the data obtained for different molecular weights to generate a master curve at each temperature, i.e., a plot corresponding to $[G''_P]_R$ and $[G'_P]_R$ versus $\omega\tau_1$, it is necessary to shift the data along the frequency axis by the longest relaxation time, τ_1, and along the vertical axis by the stress-optic coefficient, C. Values of τ_1 were obtained by direct comparison of the infinite-dilution frequency-dependent properties with the Gaussian BSM predictions. If this is done in the polar format (i.e., S_{mP} and θ_P versus $\omega\tau_1$), the results can be slightly more reliable because the phase-angle curves cannot be shifted vertically to enhance the fit (unlike S'_P or S''_P), but no significant difference was detected between the two methods for the data presented here. The resulting values have estimated uncertainties of ±5%. In Figure 3, the M dependence of τ_1 is displayed for the four temperatures examined. The data have been normalized by (T/η_s), to ensure that the observed changes in τ_1 reflect solely changes in coil dimensions and hydrodynamic interaction. At the nominal Θ temperature, 21.5 °C,[50] and at 18.0 and 25.0 °C, the exponent values ($=3\nu$) are 1.48, 1.50, and 1.51, respectively, which are in good agreement with the expected value of 1.50. The uncertainties for each of these values is ±0.02. At 21.5 °C, Colby reports an intrinsic viscosity–molecular weight relationship[25,26]

$$[\eta] = 0.0903M^{0.549} \quad (21)$$

implying the slightly larger value of 0.516 for ν. At 30 °C, in contrast, the effect of increasing temperature is clear; the τ_1 exponent increases to 1.58 ± 0.02. In a good solvent, the maximum value of this exponent should be 1.8 (actually 1.764 for ν 0.588), and so clearly at 30 °C the solvent quality is marginal.

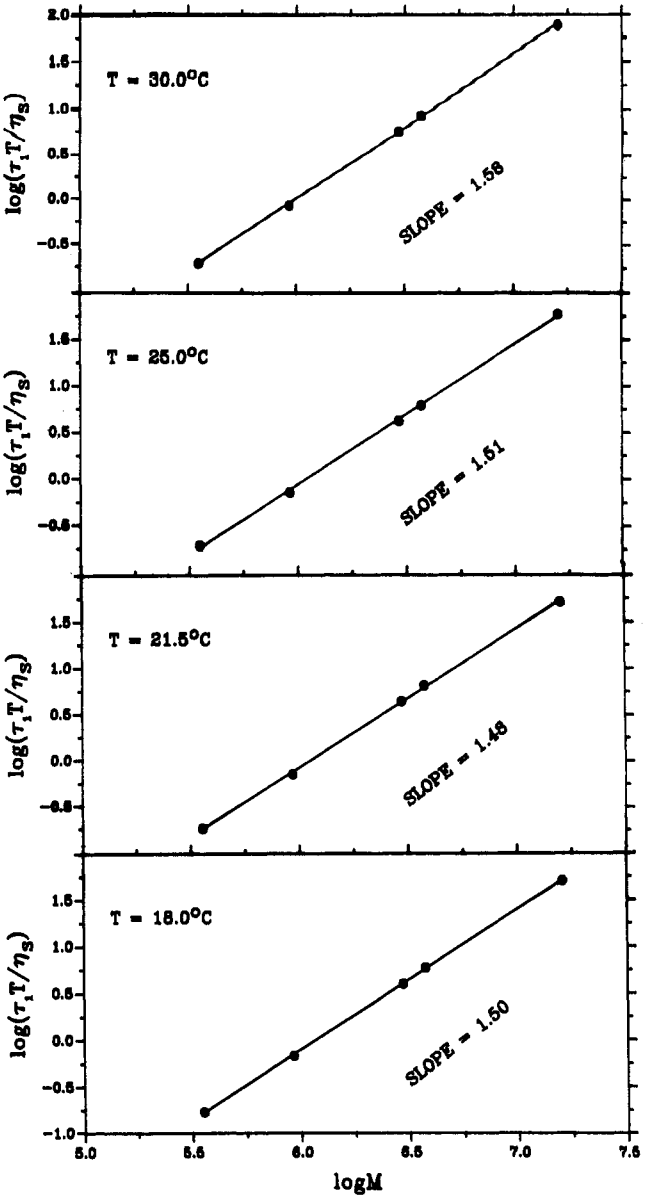

Figure 3. Infinite-dilution longest relaxation time, scaled by T/η_s, as a function of molecular weight for T = 18.0, 21.5, 25.0, and 30.0 °C.

Table III
Stress-Optic Coefficients for Polybutadiene in Dioctyl Phthalate at 21.5 °C

M_w	C, cm²/dyn	M_w	C, cm²/dyn
3.55×10^5	3.54×10^{-10}	3.74×10^6	3.18×10^{-10}
9.25×10^5	3.77×10^{-10}	1.60×10^7	3.89×10^{-10}
2.95×10^6	2.07×10^{-10}		

The second shift, along the vertical (reduced moduli) axis, requires specification of the stress-optic coefficient, C. This may be determined from the ratio of the intrinsic low-frequency limiting birefringence, $[S_{0,P}]$, to the intrinsic viscosity, obtained via eq 21, as

$$C = [S_{0,P}]/2\eta_s[\eta] \quad (22)$$

where $S_{0,P}$ is obtained as the low-frequency limiting value of $\{(S'_P)^2 + (S''_P)^2\}^{1/2}$. The values of C at 21.5 °C thus obtained are listed in Table III. Samples 1, 2, 4, and 5

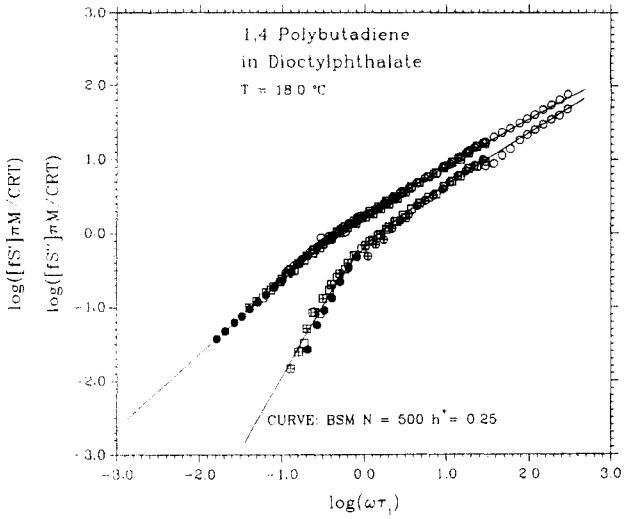

Figure 4. Infinite-dilution OFB properties at 18.0 °C, in the master plot format discussed in the text, compared to the predictions of the Gaussian bead–spring model with $h^* = 0.25$. Data for different molecular weights are indicated as follows: (●) 3.55×10^5; (⊞) 9.25×10^5; (□) 2.95×10^6 (⊕) 3.75×10^6; (○) 1.60×10^7.

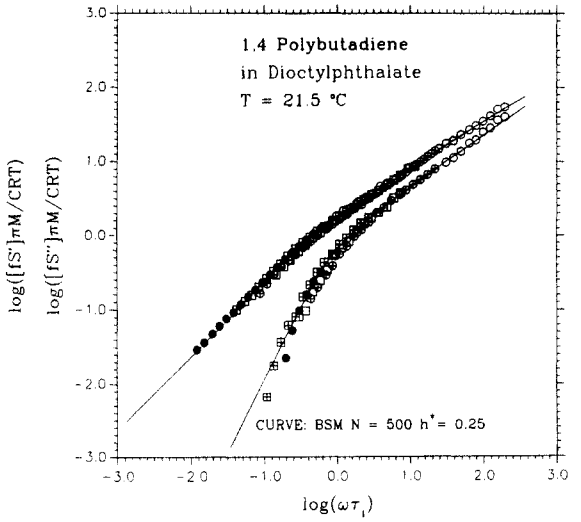

Figure 5. Infinite-dilution OFB properties at 21.5 °C, compared to the predictions of the Gaussian bead–spring model with $h^* = 0.25$. Symbols are as in Figure 4.

yield an average value for C for 3.6×10^{-10} cm²/dyn, while sample 3 has the substantially lower value of 2.1×10^{-10} cm²/dyn. In general, C is expected to be independent of M, but it certainly will depend on the details of the chain microstructure. Sample 3 is reported to have a significantly higher fraction of 1,2-PB units, and a rough calculation indicates that this could account for the lower value of C.[51] The other differences among the C values could also reflect subtle differences in microstructural composition. In any event, these values of C provide the requisite vertical shift factors for 21.5 °C. For the other temperatures, the C values were simply scaled by the expected $1/T$ dependence of C, neglecting any temperature dependence in either the polarizability anisotropy, $\alpha_1 - \alpha_2$, or the refractive index of the solvent, which is reasonable given the small temperature range involved.

A. Θ Regime. The resulting master curves for the two lower temperatures are displayed in Figures 4 and 5, plotted in a double-logarithmic format as $[fS'_P]_R$ and $[fS''_P]_R$ versus $\omega\tau_1$. The reduced birefringence "moduli" are defined by

$$[fS'_P]_R \equiv (\pi M/CRT)[fS'_P] \tag{23a}$$

$$[fS''_P]_R \equiv -(\pi M/CRT)[fS''_P] \tag{23b}$$

and are thus equivalent to $[G''_P]_R$ and $[G'_P]_R$, respectively. In general, the superpositions are excellent, with slightly more scatter evident in the elastic components. The results obtained at 18.0 and 21.5 °C are both compared with the BSM predictions with $h^* = 0.25$. The agreement is excellent in both cases. The fact that the results are indistinguishable for these two distinct temperatures reflects a combination of two effects. First, conformational dynamics in general are not the most sensitive way to detect subtle changes in solvent quality, compared to the second virial coefficient, for example. Second, for finite M one expects a finite Θ temperature interval, rather than a single Θ point.

It should be reemphasized that once τ_1 and C have been determined, there are no adjustable parameters in this comparison between experiment and theory. Theoretical curves generated from the uniform expansion model with $\epsilon = 0$, from the blob model with $N_\tau \to \infty$, and from the RG model with $z = 0$ are identical, when h^* is fixed at 0.25. The value of $N = 500$ in Figure 5 is arbitrary, in the sense that the frequency range shown is not sufficient to reveal evidence of an apparent "end" to the relaxation spectrum (i.e., $\omega\tau_N \approx 1$), and thus curves for any large N would superpose. This is marked contrast to infinite-dilution results for polystyrene in Aroclor solvents, which require the use of specific, finite values of N to describe the data over the accessible frequency range.[10-17] This difference is due, inter alia, to the large difference (ca. 10^4) in solvent viscosities involved.

The present results demonstrate for the first time that the BSM provides an excellent description of the infinite-dilution OFB properties of flexible chains in a Θ solvent, in accordance with the known results for the VE properties. In Figure 6, the data of Figure 5 are replotted as open circles, and the VE results for PS in decalin obtained by Hair and Amis are shown as filled circles.[21] The agreement between the two different experiments, on two different polymer/solvent systems, is very good; the advantage of a continuously variable drive frequency in the OFB instrumentation is also apparent.

In Figure 7, the data of Figure 5 for 21.5 °C are again replotted and compared with the dynamical scaling predictions (eqs 20a and 20b) for $\omega\tau_1 > 1$ with $\nu = 0.5$. The agreement is excellent for $[fS'_P]_R$ and quite reasonable for $[fS''_P]_R$. Dynamic scaling actually makes three separate predictions for the plotted quantities, namely, the magnitudes, slopes, and relative separation of the two functions. Clearly, the slopes and relative separation are well-described; however, an arbitrary vertical shift of 0.03 has been applied to bring the predictions into agreement with the data. However, this relatively small correction may reflect uncertainty in the value of C more than any inadequacy in eqs 20a and 20b. A best fit to the $[fS'_P]_R$ data for $\omega\tau_1 > 3$ gives a slope of $1/3\nu = 0.68 \pm 0.02$, compared to the prediction of 0.67 and consistent with $\nu = 0.493$ for the M dependence of τ_1 shown in Figure 3.

B. Marginal Regime. In the following section, the discussion is confined to the data at 30 °C, where the effects of excluded volume are most evident. The results at 25 °C are not presented here in the interest of brevity but are discussed elsewhere;[51] in general, the 25 °C results are intermediate between those obtained at 21.5 °C and those at 30 °C, as expected. In Figures 8–12, the master curves for 30 °C are shown in the same format as those in Figures

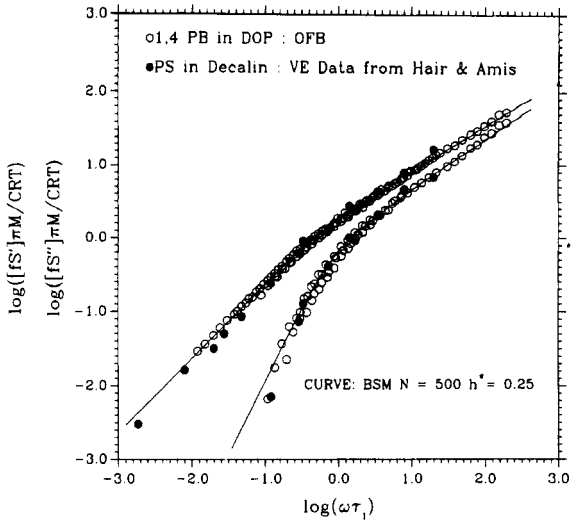

Figure 6. Infinite-dilution OFB properties as in Figure 5, compared to the viscoelastic properties for polystyrene/decalin, from ref 21.

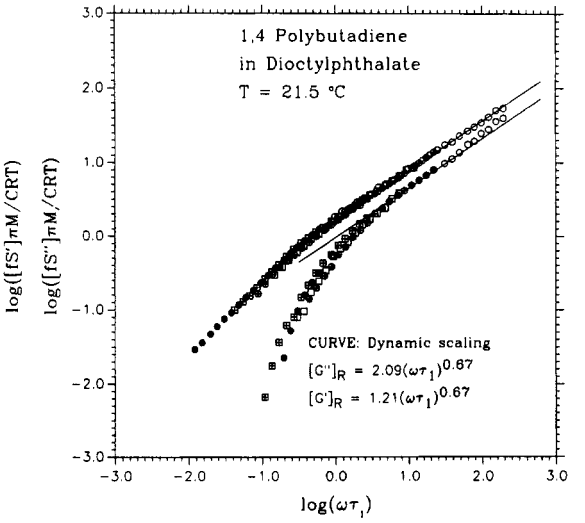

Figure 7. Infinite-dilution OFB properties as in Figure 5, compared to the dynamic scaling predictions with $\nu = 0.500$.

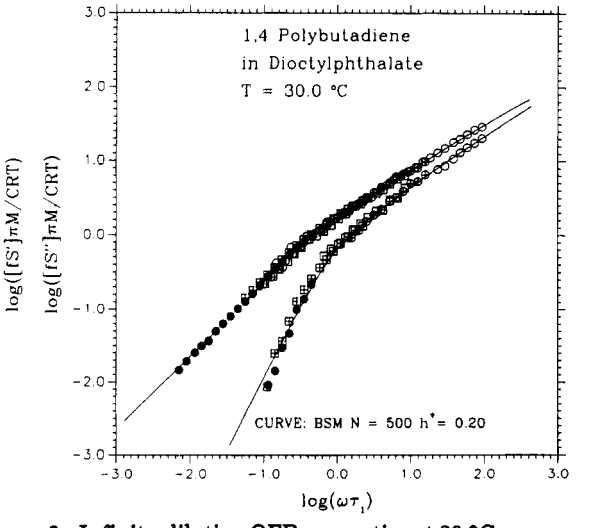

Figure 8. Infinite-dilution OFB properties at 30 °C, compared to the predictions of the Gaussian bead–spring model with $h^* = 0.20$. Symbols are as in Figure 4.

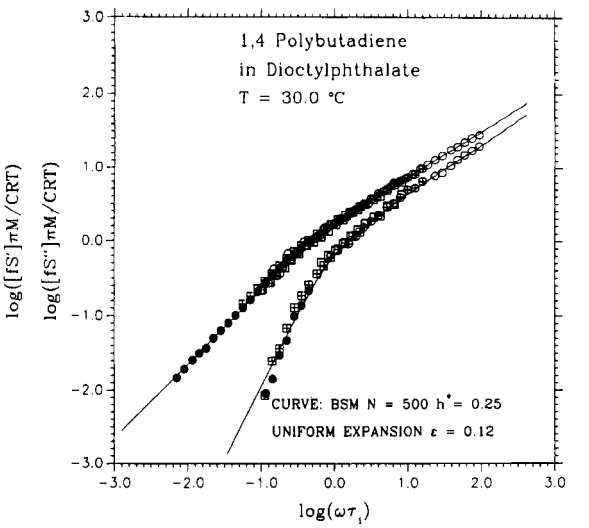

Figure 9. Infinite-dilution OFB properties as in Figure 8, compared to the predictions of the uniform expansion bead–spring model with $\epsilon = 0.12$ and $h^* = 0.25$.

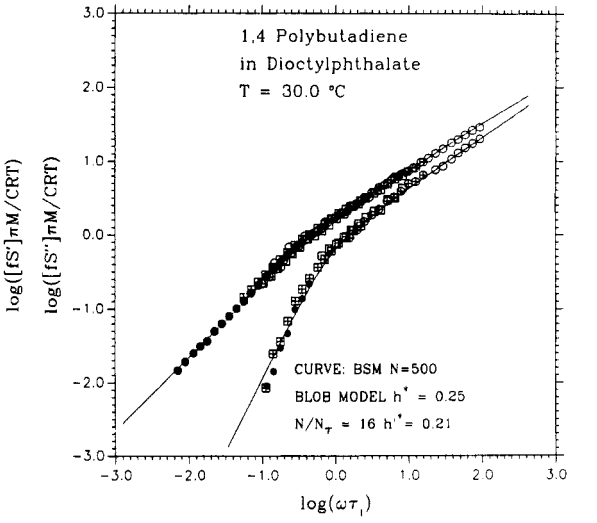

Figure 10. Infinite-dilution OFB properties as in Figure 8, compared to the predictions of the blob bead–spring model with $N/N_\tau = 16$, $h^* = 0.25$, and $h^{*\prime} = 0.21$.

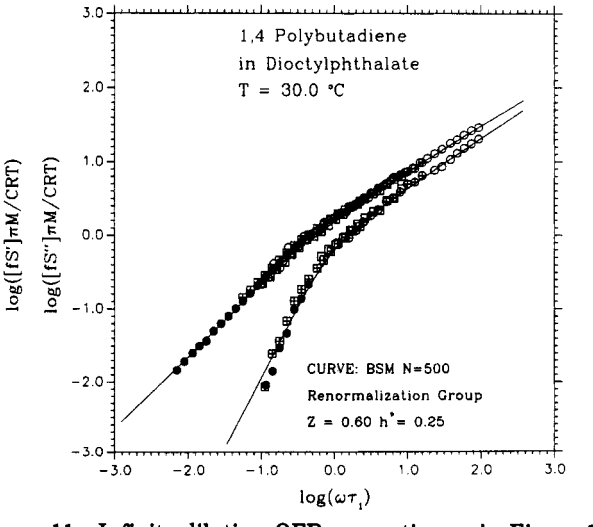

Figure 11. Infinite-dilution OFB properties as in Figure 8, compared to the predictions of the renormalization group bead–spring model with $z = 0.60$ and $h^* = 0.25$.

4–7 and compared to the BSM predictions using variable h^* (Figure 8), uniform expansion (Figure 9), the blob model (Figure 10), the RG theory (Figure 11), and dynamic scaling (Figure 12). In all cases the theoretical curves describe the data very well, and thus the important issue is to compare the self-consistency of the various parameter values. This may be done in the following manner. The

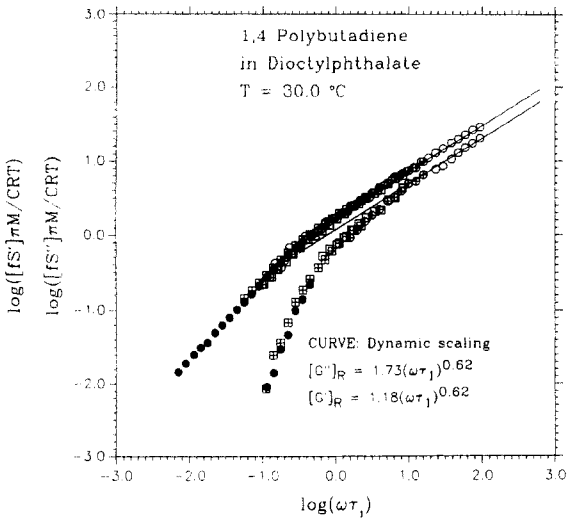

Figure 12. Infinite-dilution OFB properties as in Figure 8, compared to the dynamic scaling predictions with $\nu = 0.538$.

effects of excluded volume should be manifest in at least three ways: the slope of the data in the high-frequency regime, the M dependence of τ_1, and the T dependence of $[S_{0,P}]$. The M dependence of $[S_{0,P}]$ should be equivalent to that of τ_1. The fits in Figures 8–12 have been selected to optimize the agreement with the data in terms of the high-frequency slope, and consequently self-consistency may be assessed using the other two criteria.

For 30 °C, the M exponent for τ_1 is 1.58 ($\nu = 0.527$). In comparison, the M exponent for $[S_{0,P}]$ is 0.62 ($\nu = 0.540$), which is slightly different but certainly confirms the onset of excluded-volume effects. Note that $[S_{0,P}]$ is directly proportional to $[\eta]\eta_s/T$, from eqs 3 and 22. The T dependence of $[S_{0,P}]T/\eta_s$, therefore, can be used to establish an expansion factor, α, corresponding to the intrinsic viscosity expansion factor, α_η. This factor will depend on M. As the highest M sample examined contributes the most to the high-frequency regime in Figures 8–12, it is the corresponding value of α that is of most relevance. This was determined to be 1.17, using the data at 21.5 °C as the reference. (An additional subtlety should be mentioned here, that in principle it should not be possible to obtain a perfect master curve in the marginal solvent regime. The reason is that different M samples will experience different degrees of swelling, such that the spacings of the relaxation times relative to the longest time will vary with M. However, the finite frequency range covered for a single M, combined with the generally weak effect of excluded volume on the relaxation spectrum, obviates this difficulty.)

In Figure 8, a value of $h^* = 0.20$ has been used to obtain the best fit. Hair and Amis[21,22] have shown that there is a direct correspondence between the Mark–Houwink–Sakurada exponent, a ($=3\nu - 1$), and the value of h^*, by direct computation of the exact eigenvalues of the BSM for large values of N. Thus, a varies smoothly from 0.5, when $h^* = 0.25$, to 1, when $h^* = 0$, for the Gaussian chain. A value of $h^* = 0.20$ is equivalent to $a \approx 0.53$, which should correspond to an exponent of 1.53 for the M dependence of τ_1, or 0.53 for $[S_{0,P}]$. However, as noted above, the actual exponents are 1.58 and 0.62, respectively, and thus the BSM with variable h^* does not provide a completely self-consistent description of these data. It would take a value of $h^* = 0.13$ to correspond to $a = 0.58$, which is beyond the uncertainty in fitting the data in Figure 8.

In Figure 9, a uniform expansion exponent of $\epsilon = 0.12$ has been employed, with h^* maintained at 0.25. The self-consistency of this value may be assessed in two ways. One route is to equate ϵ with $2\nu - 1$, corresponding to $\nu = 0.56$, and thus to τ_1 and $[S_{0,P}]$ exponents of 1.68 and 0.68, respectively; these values are clearly larger than those observed. Another incorporates the expression of Stockmayer and Fixman:[52]

$$\epsilon = (\alpha^3 - 1)/(3\alpha^3 - 0.674) \tag{24}$$

leading to $\alpha = 1.13$, in reasonable agreement with the experimental estimate of 1.17. The uniform expansion approach could also be employed with values of h^* less than 0.25; in this way, ϵ could be reduced to bring the value of ν into agreement with the experimental results. However, then eq 24 would yield an even lower value for α. Thus, there is some doubt as to whether the uniform expansion model can describe the data self-consistently; but, given the uncertainty in determining the best experimental value of ϵ, the data by themselves do not eliminate the uniform expansion model as a viable approach.

In Figure 10, the data are compared to the BSM incorporating the blob model, with a value of $N/N_\tau = 16$ ($N_\tau \approx 30$). The value of h^* has been maintained at 0.25 for short length scales ($|i - j| < N_\tau$) but decreased to $h^{*\prime} = 0.21$ for long length scales, for the reason described previously. The close correspondence between the data and the model predictions indicates that it is not necessary to use the modified blob model in this case; the artificial discontinuity in the range of the excluded-volume interaction is not apparent in the relaxation spectrum, once the two h^* values are employed. To access the self-consistency of the fit, an expression given by Weill and des Cloiseaux[53] can be used:

$$\alpha_\eta = 0.86(N/N_\tau)^{0.1} \tag{25}$$

For the selected value of (N/N_τ), eq 25 gives $\alpha = 1.13$, again in reasonable agreement with the experimental value of 1.17. In fact, if α were set to 1.17, eq 25 would give $(N/N_\tau) = 22$, which would not result in an appreciable change in the quality of the fit in Figure 10. Thus, the incorporation of the blob model appears to provide a successful and numerically straightforward means to incorporate the effects of variations in solvent quality in the BSM.

In Figure 11, the data are compared to the RG model, using a value of $z = 0.60$ and with h^* again held at 0.25. As with the preceding cases, the agreement between experiment and theory is excellent. A value for z can be estimated by the formula for the expansion factor:[47]

$$\alpha_\eta^3 = (1 + 6.44z)^{3/8}[1 - 0.276(6.44z/1 + 6.44z)], \quad z \leq 0.75 \tag{26}$$

Insertion of $z = 0.60$ in eq 26 gives an estimate for α of 1.12, again in reasonable agreement with the experimental value. The value of z corresponds to $\nu = 0.57$ by eq 18, which is slightly larger than the values obtained experimentally. As with the uniform expansion and blob model cases, the data have been well-described without varying h^* from the non-free-draining limit of 0.25. This is in agreement with the conclusion of Hair and Amis, who were able to describe viscoelastic properties in the good solvent limit (polystyrene in toluene) using the RG model and $h^* = 0.25$.[22]

The principal conclusions from Figures 8–11 and the preceding discussion are that (i) any of the four approaches to modifying the BSM are capable of describing the frequency dependence of the reduced moduli extremely well, (ii) the Gaussian BSM with variable h^* is the least able to describe the effects of excluded volume in a self-

Table IV
Parameter Values for Polybutadiene in Dioctyl Phthalate at 30.0 °C

	ν	α
experiment	0.533	1.17
Gaussian BSM with $h^* = 0.20$	0.51	
uniform expansion with $\epsilon = 0.12$	0.56	1.13
blob model with $N_\tau = 30$		1.13
renormalization group with $z = 0.60$	0.57	1.12

consistent way, (iii) conformational dynamics experiments in the intermediate solvent quality regime cannot discriminate among the various treatments of excluded volume, (iv) the RG satisfies the self-consistency criterion at least as well as do the other approaches, and, in view of its overall success in describing the static and dynamic properties of flexible chains, is to be preferred, and (v) once excluded-volume effects are incorporated through $\langle r_{ij}^{-1} \rangle$, it is no longer necessary to vary h^*. However, it remains an interesting question as to whether in principle h^* should be varied or not.[54] In Table IV, the experimental values of ν and α are compared with those inferred from the various models. In general, the fits in Figures 9–11 correspond to values of α which are systematically slightly below those obtained experimentally. However, the experimental value of 1.17 was determined for the largest M studied, since these data extended to the highest frequencies. The α values for the next three lower molecular weights have an average of 1.09, and the data for these samples do contribute to the high-frequency regime in Figures 8–12. From this perspective, then, the apparent systematic deviation is quite understandable; the value of $\alpha \approx 1.13$ implied by the various fits is consistent with a weighted average of the experimentally determined values. The variation of α with M also underscores the fact that data in the intermediate solvent quality regime should not, in fact, superpose exactly.

The data have been compared to the dynamic scaling expressions in figure 12. In this case, the slopes and relative separation of the two functions at high frequency are well-described by eqs 20a and 20b with $\nu = 0.54$. In contrast to Figure 7, no vertical shift was needed to bring the scaling lines into numerical agreement with the data. This value of ν is in good agreement with the values obtained from the M dependences of τ_1 and $[S_{0,P}]$ discussed above. The slope of 0.62 is approximately halfway between the Θ solvent value, 0.67, and the good solvent limit of 0.565. The success of the dynamic scaling approach is appealing, in the sense that it provides a simple mechanism for estimating the relaxation spectrum of flexible chains in solvents of arbitrary quality, without recourse to exact numerical computation of the BSM eigenvalues. It is interesting to compare the dynamic scaling approach with infinite-dilution OFB data obtained in a better solvent system, PS/Aroclor 1248. The highest M for which such data are available is 1.8×10^6.[17] The results are shown in Figure 13. First, it is important to note that the data have been truncated at high frequency to remove the finite N effects alluded to previously. Second, the data have been obtained at several temperatures and reduced to 25 °C via time–temperature superposition. The slopes and relative separations are again well-described, this time with $\nu = 0.56$, indicating that the PS/Aroclor system is of intermediate thermodynamic quality, as claimed previously,[14] but certainly closer to good solvent conditions than is PB/DOP at 30 °C. These results also confirm that the PS/Aroclor system displays universal features in the internal dynamics, at least for effective drive frequencies that are not too high. Exactly how "too high" should be defined

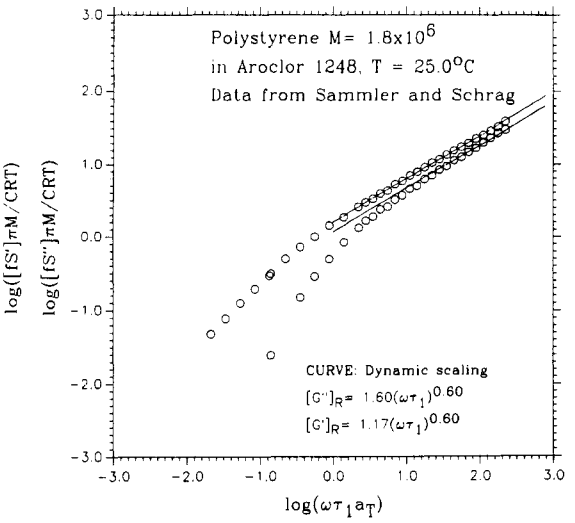

Figure 13. Infinite-dilution OFB properties for polystyrene ($M = 1.8 \times 10^6$) in Aroclor 1248 from ref 17, compared to the dynamic scaling predictions with $\nu = 0.556$.

remains as an intriguing problem, but one which is beyond the scope of this paper.

Summary

The infinite-dilution oscillatory flow birefringence (OFB) properties of five high molecular weight polybutadiene samples have been determined in dioctyl phthalate, near and just above the Θ temperature. The data acquired at each temperature have been superposed to form master curves corresponding to the reduced intrinsic shear moduli, $[G'_P]_R$ and $[G''_P]_R$, plotted as functions of the reduced frequency, $\omega\tau_1$, in a double-logarithmic format. The superposition along the vertical axis is achieved via the stress-optical relation, whereas the horizontal shift factor is the longest relaxation time, τ_1. The resulting master curves, which generally extend over 4 decades in reduced frequency and up to $\omega\tau_1 \approx 10^2$, have been compared to the predictions of the bead–spring model (BSM) using five approximate schemes for incorporating the effects of excluded volume. These include (i) the original BSM of Rouse and Zimm, with variable hydrodynamic interaction (h^*), (ii) the uniform expansion approach of Peterlin, as incorporated by Tschoegl, (iii) the blob model of Farnoux et al. and Akcasu et al., (iv) the renormalization group theory of Miyake and Freed, as incorporated by Sammler and Schrag, and (v) the dynamic scaling approximation of Doi and Edwards. Methods ii–iv incorporate the Ptitsyn–Eizner approach, in that excluded volume enters the calculation of the eigenvalues of the BSM through the mean inverse bead separation, $\langle r_{ij}^{-1} \rangle$.

For these solutions at 18 and 21.5 °C, in the Θ regime, methods i–iv yield identical results, and the data are described very well with $h^* = 0.25$. This is in agreement with viscoelastic measurements reported by several groups, but it represents the first time to our knowledge that the infinite-dilution OFB properties have been obtained in a Θ system. The dynamic scaling approach also works well in this regime.

For the data obtained at 30 °C, the effects of excluded volume are evident. Again, all five methods are capable of describing the frequency dependence of the reduced intrinsic moduli extremely well; however, some interesting differences emerge. In each case, the relevant parameter is adjusted to obtain the best agreement with the data in terms of the slopes and relative separation of the two

moduli at high frequencies. For self-consistency, the resulting parameter values should also describe the molecular weight dependences of τ_1 and the low-frequency limiting intrinsic birefringence, $[S_{0,P}]$, at the particular temperature, in addition to the expansion factor of the chain determined from the temperature dependence of $[S_{0,P}]$. By this criterion method i is the weakest, although a value of $h^* = 0.20$ describes the frequency dependence well. Methods ii–iv all satisfy the self-consistency criterion to a reasonable degree, with respective parameter values of $\epsilon = 0.12$, $N/N_\tau = 16$, and $z = 0.60$. In all three cases, h^* was fixed at the non-free-draining limit of 0.25, indicating that it is not necessary to vary this parameter at all. However, it would certainly be possible to fit the data equally well by varying h^* slightly, in addition to the excluded-volume parameters. Thus, these data do not establish or refute the concept of "partial draining". It is not possible to discriminate among these approaches on the basis of the OFB data alone, but in terms of the solution properties of flexible polymers taken as a whole, the renormalization group approach is clearly to be preferred. In particular, in this manifestation, z is the only additional parameter required in the BSM and concurrently permits direct connection with previous dynamic and thermodynamic measurements on polymer solutions. Finally, the success of the dynamic scaling approach suggests that it can provide an excellent approximation for the relaxation spectrum of an isolated flexible chain under any solvent conditions, without numerical calculation of the eigenvalues.

Over the years the BSM has proven to be remarkably successful in describing the conformational dynamics properties of flexible polymers. However, there have been at least three major limitations to its utility: the failure to account for excluded volume, the failure to describe shear thinning and other finite strain/strain rate rheological properties, and the failure to represent dynamics accurately at the segmental and monomer level. We feel that the incorporation of the renormalization group into the BSM, albeit in an approximate fashion, effectively removes the first of these three shortcomings.

Acknowledgment. This work was supported by the National Science Foundation, through Grants DMR-8715391 and DMR-9018807. The assistance of Dr. S. Amelar with the OFB measurements is greatly appreciated. We thank Dr. R. L. Sammler for generously providing computer programs and Drs. R. H. Colby and L. J. Fetters for generously providing the polymer samples. Helpful discussions with Drs. S. Amelar, E. J. Amis, R. H. Colby, J. F. Douglas, K. F. Freed, and J. L. Schrag are also acknowledged.

References and Notes

(1) Rouse, P. E., Jr. *J. Chem. Phys.* **1953**, *21*, 1872.
(2) Zimm, B. H. *J. Chem. Phys.* **1956**, *24*, 269.
(3) Ptitsyn, O. B. *Zh. Fiz. Khim.* **1957**, *31*, 1091. Ptitsyn, O. B.; Eizner, Y. E. *Zh. Fiz. Khim.* **1958**, *32*, 2464. Eizner, Y. E.; Ptitsyn, O. B. *Vysokomol. Soedin.* **1962**, *4*, 1725.
(4) Peterlin, A. *J. Chem. Phys.* **1955**, *23*, 2464.
(5) Tschoegl, N. W. *J. Chem. Phys.* **1963**, *39*, 149; **1964**, *40*, 473.
(6) Miyake, A.; Freed, K. F. *Macromolecules* **1983**, *16*, 1228; **1984**, *17*, 678.
(7) Sammler, R. L.; Schrag, J. L. *Macromolecules* **1988**, *21*, 3273; **1989**, *22*, 3435.
(8) Thurston, G. B.; Peterlin, A. *J. Chem. Phys.* **1967**, *46*, 4881. Thurston, G. B.; Morrison, J. D. *Polymer* **1969**, *10*, 421.
(9) Ferry, J. D. *Viscoelastic Properties of Polymers*, 3rd ed.; Wiley: New York, 1980; and references therein.
(10) Lodge, T. P.; Miller, J. W.; Schrag, J. L. *J. Polym. Sci., Polym. Phys. Ed.* **1982**, *20*, 1409.
(11) Lodge, T. P.; Schrag, J. L. *Macromolecules* **1982**, *15*, 1376.
(12) Landry, C. J. T. Ph.D. Thesis, University of Wisconsin, 1985.
(13) Sammler, R. L.; Landry, C. J. T.; Woltman, G. R.; Schrag, J. L. *Macromolecules* **1990**, *23*, 2388.
(14) Amelar, S.; Eastman, C. E.; Morris, R. L.; Smeltzly, M. A.; Lodge, T. P.; von Meerwall, E. D. *Macromolecules* **1991**, *24*, 3505.
(15) Soli, A. L.; Schrag, J. L. *Macromolecules* **1979**, *12*, 1159.
(16) Dibbs, M. G. Ph.D. Thesis, University of Wisconsin, 1983.
(17) Sammler, R. L. Ph.D. Thesis, University of Wisconsin, 1985.
(18) Strand, D. A. Ph.D. Thesis, University of Wisconsin, 1989.
(19) Johnson, R. M.; Schrag, J. L.; Ferry, J. D. *Polym. J.* **1970**, *1*, 742.
(20) Tanaka, H.; Sakanishi, A.; Kaneko, M.; Furuichi, J. *J. Polym. Sci., Part C* **1966**, *15*, 317.
(21) Hair, D. W.; Amis, E. J. *Macromolecules* **1989**, *22*, 4528.
(22) Hair, D. W.; Amis, E. J. *Macromolecules* **1990**, *23*, 1889.
(23) Doi, M.; Edwards, S. F. *The Theory of Polymer Dynamics*; Oxford University Press: Oxford, U.K., 1986.
(24) Birnboim, M. H.; Elyash, L. *J. Bull. Am. Phys. Soc.* **1966**, *11*, 165. Schrag, J. L.; Johnson, R. M. *Rev. Sci. Instrum.* **1971**, *42*, 224.
(25) Colby, R. H. Ph.D. Thesis, Northwestern University, 1985.
(26) Colby, R. H.; Fetters, L. J.; Funk, W. G.; Graessley, W. W. *Macromolecules* **1991**, *24*, 3873.
(27) Colby, R. H.; Fetters, L. J.; Graessley, W. W. *Macromolecules* **1987**, *20*, 2226.
(28) Miller, J. W.; Schrag, J. L. *Macromolecules* **1975**, *8*, 361.
(29) Morris, R. L.; Lodge, T. P. *Anal. Chim. Acta* **1986**, *189*, 183.
(30) Man, V. F. Ph.D. Thesis, University of Wisconsin, 1984.
(31) Merchak, P. A. Ph.D. Thesis, University of Wisconsin, 1987.
(32) Stokich, T. M., Jr. Ph.D. Thesis, University of Wisconsin, 1988.
(33) Morris, R. L.; Amelar, S.; Lodge, T. P. *J. Chem. Phys.* **1988**, *89*, 6523.
(34) Schrag, J. L.; Stokich, T. M.; Strand, D. A.; Merchak, P. A.; Landry, C. J. T.; Radtke, D. R.; Man, V. F.; Lodge, T. P.; Morris, R. L.; Hermann, K. C.; Amelar, S.; Eastman, C. E.; Smeltzly, M. A. *J. Non-Cryst. Solids* **1991**, *131–133*, 537.
(35) Amelar, S.; Krahn, J. R.; Hermann, K. C.; Morris, R. L.; Lodge, T. P. *Spectrochim. Acta Rev.* **1991**, *14*, 379.
(36) Extensive references to the phenomenology of the high-frequency limiting viscosity, designated η'_∞, and related quantities may be found in refs 31–35.
(37) See, for example: Janeschitz-Kriegl, H. *Adv. Polym. Sci.* **1969**, *6*, 170.
(38) Lodge, A. S.; Wu, Y.-J. *Rheol. Acta* **1971**, *10*, 539.
(39) Kirkwood, J. G.; Riseman, J. *J. Chem. Phys.* **1948**, *16*, 565.
(40) Daoud, M. Ph.D. Thesis, Universite de Paris VI, 1977. Farnoux, B.; Boue, F.; Cotton, J. P.; Daoud, M.; Jannink, G.; Nierlich, M.; de Gennes, P.-G. *J. Phys. (Paris)* **1978**, *39*, 77.
(41) Akcasu, A. Z.; Benmouna, M.; Alkhafaji, S. *Macromolecules* **1981**, *14*, 147.
(42) Flory, P. J. *Principles of Polymer Chemistry*; Cornell University Press: Ithaca, NY, 1953.
(43) Osaki, K. *Adv. Polym. Sci.* **1973**, *12*, 1.
(44) Yamakawa, H. *Modern Theory of Polymer Solutions*; Harper and Row: New York, 1971.
(45) Freed, K. F., personal communication.
(46) Douglas, J. F.; Freed, K. F. *Macromolecules* **1985**, *18*, 201.
(47) Freed, K. F. *Renormalization Group Theory of Macromolecules*; Wiley-Interscience: New York, 1987.
(48) Freed, K. F.; Douglas, J. F. *J. Chem. Phys.* **1988**, *88*, 2764.
(49) de Gennes, P.-G. *Scaling Concepts in Polymer Physics*; Cornell University Press: Ithaca, NY, 1979.
(50) In ref 25, 21.5 °C was identified as T_θ for PB/DOP, but in ref 26, a new estimate of ca. 13 °C was given. There is thus some ambiguity in the exact value of T_θ for this system. We found that our solutions routinely turned cloudly below 15–16 °C and therefore doubt that 13 °C is a good estimate for our solutions; 21.5 °C appears to be a more reasonable estimate based on our results. For our measurements, DOP was exhaustively washed and then vacuum distilled, as discussed in the Experimental Section, and thus there could be slight differences in chemical composition (i.e., impurities) between our solvent and that used in refs 25 and 26. In any event, the data analysis presented in this paper does not depend critically on a precise specification of T_θ.
(51) Sahouani, H. Ph.D. Thesis, University of Minnesota, 1991.
(52) Stockmayer, W. H.; Fixman, M. *J. Polym. Sci.* **1963**, *1*, 137.
(53) Weill, G.; des Cloizeaux, J. *J. Phys. (Paris)* **1979**, *40*, 99.
(54) Douglas, J. F., personal communication.

Registry No. PB (homopolymer), 9003-17-2; DOP, 117-81-7.